

Numerical Investigation of Flow Modification Drag Reduction Technique Using Sharp Spike and Counter Flow Jet of Blunt Body in Hypersonic Flow

Shyam Singh Kanwar^{1*}, Gajendra Kumar Agrawal², Sandip Kumar Sahu³, Uday Khakha⁴, Satish Kumar Gavel⁵, Avinash Ranjan Patnaik⁶, Sharda Pratap Shrivastava⁷

^{1*,2,3,4,5,6}Department of Mechanical Engineering, Government Engineering College Bilaspur, Chhattisgarh, India

⁷Department of Mechanical Engineering, Chouksey Engineering College Bilaspur, Chhattisgarh, India

***Corresponding Author:** Shyam Singh Kanwar

*Email: shyamkanwar@gecbasp.ac.in

ABSTRACT

This research paper presents a comprehensive analysis of air injection at the tip of an aerospike on a blunt body using numerical simulation techniques. Aerospikes are employed to modify the shock wave structure and improve the aerodynamic performance of blunt bodies, which are commonly used in high-speed aerospace applications. The study aims to explore the potential benefits of integrating air injection at the aerospike tip to further enhance drag reduction and flow stability. Using advanced computational fluid dynamics (CFD) simulations using ANSYS Fluent Software, the study investigates the effects of various air injection parameters such as injection pressure, on the flow field and aerodynamic characteristics of the blunt body-aerospike configuration. The numerical simulations are validated against available experimental data and standard empirical correlations to ensure accuracy and reliability. The results indicate that air injection at the aerospike tip significantly influences the shock wave pattern, resulting in a notable reduction in aerodynamic wave drag. The optimal air injection parameters were identified, showing a drag reduction improvement of up to 71% compared to a conventional aerospike without air injection. Here, air is injected from tip of the sharp spike. In this analysis, various jet (opposing) inlet conditions with different pressure ratios have been investigated. The studies have been done for 2 L/D ratios namely for 0.2 and 1. The steady, compressible, Navier-Stokes equations are solved with classic SST (Shear Stress Transport) turbulent flow model for zero angle of attack at Mach number 8. Furthermore, the analysis reveals that air injection enhances the stability of the flow field by mitigating flow separation and reducing pressure oscillations around the blunt body. The findings of this study underscore the potential of air injection at the aerospike tip as an effective method for improving the aerodynamic performance and stability of blunt bodies in high-speed flight conditions. The insights gained from the numerical simulations provide a valuable foundation for the development of advanced aerospace vehicle designs. Future research will focus on refining the air injection strategies and extending the analysis to different aerodynamic configurations and flight regimes.

Keywords: Aerospike, Air Injection, Blunt Body, Numerical Simulation, Drag Reduction, Shock Wave Modification

1. Introduction

The aerodynamic performance of blunt bodies in high-speed flight remains a cornerstone of aerospace engineering, particularly for re-entry vehicles and supersonic aircraft. These designs are favored for their thermal protection properties, as they generate strong bow shocks that effectively dissipate heat [1]. However, these shock waves also induce significant aerodynamic drag, impairing overall vehicle performance [2]. To address this issue, various methods have been explored, with aerospikes emerging as effective passive flow control devices [3]. Aerospikes are utilized to modify the shock wave structure and reduce drag by displacing the shock wave away from the blunt body [4]. Extensive research, both experimental and numerical, has demonstrated the benefits of aerospikes in reducing drag and heat flux [5-8]. For instance, recent studies by Smith et al. [9] and Zhao et al. [10] have shown considerable reductions in drag at various Mach numbers using aerospikes. Beyond passive methods, active flow control techniques such as air injection have shown significant promise in enhancing aerodynamic performance [11]. Air injection, which involves introducing a controlled flow of air into the freestream, can dynamically manipulate shock waves and boundary layers more effectively than passive devices [12]. Recent investigations by Marren et al. [13] and Olson et al. [14] have highlighted the potential of air injection at the aerospike tip to achieve substantial improvements in drag reduction and flow stability. Numerical simulations, particularly through computational fluid dynamics (CFD), have become indispensable in aerospace research for analysing complex flow phenomena that are challenging to capture experimentally [15-18]. Recent advancements in CFD have enabled more precise modelling of supersonic and hypersonic flows, facilitating detailed studies of the interactions between air injection and shock wave structures [19-21]. Despite the promising results of air injection strategies, there is a lack of comprehensive studies combining air injection with aerospikes on blunt bodies using numerical simulations [22]. For instance, recent work by Chen et al. [23] and Li et al. [24] has demonstrated the accuracy of CFD in predicting flow behaviour's in high-speed conditions. Despite the promising results of air injection strategies, there is a lack of comprehensive studies that combine air injection with aerospikes on

blunt bodies using numerical simulations [25]. This research aims to fill this gap by conducting a detailed numerical analysis of air injection at the tip of an aerospike on a blunt body. Specifically, the study investigates the effects of varying injection parameters, such as mass flow rate, injection angle, and injection pressure, on the aerodynamic performance and flow characteristics of the configuration. This research aims to fill this gap by conducting a detailed numerical analysis of air injection at the tip of an aerospike on a blunt body. Specifically, the study investigates the effects of varying injection parameters, such as mass flow rate, injection angle, and injection pressure, on the aerodynamic performance and flow characteristics of the configuration.

The objectives of this study are threefold:

1. To quantify the drag reduction achieved through air injection at the aerospike tip.
2. To analyse the impact of air injection on shock wave patterns and flow stability.
3. To identify the optimal air injection parameters for maximizing aerodynamic efficiency.

By addressing these objectives, this research seeks to advance the understanding of active flow control techniques in high-speed aerodynamics and provide insights for the development of more efficient aerospace vehicle designs.

2. Methodology

2.1 Governing Equations

The numerical simulation of the flow field around the blunt body with an aerospike and air injection is based on solving the Reynolds-Averaged Navier-Stokes (RANS) equations. These equations describe the conservation of mass, momentum, and energy in a compressible fluid flow:

Continuity Equation:

$$\nabla \cdot (\rho \mathbf{v}) = 0 \quad (1)$$

Momentum Equation:

$$\nabla \cdot (\rho \mathbf{v} \mathbf{v}) = -\nabla p + \nabla \cdot \mu [(\nabla \mathbf{v}) - \frac{2}{3} \nabla \cdot \mathbf{v} \mathbf{I}] \quad (2)$$

Energy Equation:

$$\nabla \cdot (\mathbf{v}(\rho E + p)) = \nabla \cdot (k_{eff} \nabla T + (\mu_{eff} [(\nabla \mathbf{v}) - \frac{2}{3} \nabla \cdot \mathbf{v} \mathbf{I}] \cdot \mathbf{v})) \quad (3)$$

Where ρ is the density, \mathbf{u} is the velocity vector, p is the pressure, μ is the dynamic viscosity, E is the total energy, k_{eff} is the thermal conductivity, and T is the temperature [26] [27].

2.2 Turbulence Model: k- ω Model

To accurately capture the turbulent effects in the high-speed flow around the blunt body with an aerospike, the k- ω (k- ω) turbulence model is employed. The k- ω model is a two-equation model that solves for the turbulence kinetic energy (k) and the specific dissipation rate (ω). The transport equations for k and ω are:

Turbulence Kinetic Energy (k) Equation:

$$\nabla \cdot (\rho k \mathbf{v}) = P_k - \beta^* \times \rho \omega k + \nabla \cdot [(\mu + \mu_k \mu_t) \nabla k] \quad (4)$$

Specific Dissipation Rate (ω) Equation:

$$\nabla \cdot (\rho \omega \mathbf{v}) = \frac{\alpha}{v_t} P_k - \beta \times \rho \omega^2 + \nabla \cdot [(\mu + \mu_\omega \mu_t) \nabla \omega] \quad (5)$$

Where P_k is the production of turbulence kinetic energy, μ_t is the eddy viscosity, and α , β , β^* , μ_k , and μ_ω are model coefficients [28] [29].

2.3 Physical model

In this paper, a 60-degree blunted cone is considered with a sharp spike at the nose region as shown in Fig.1. The geometry consists of two parts: the fore body and the after body. Figure 1(a) represents the 60-degree blunted cone as the fore body, and Figure 1(b) depicts the body with a sharp spike as the after body. In this study, a half-body was used for simulation to save computational time. The geometry of the fore body was adopted from reference Menezes *et al* [40], while the after body geometry was sourced from reference Ahmed *et al* [41].

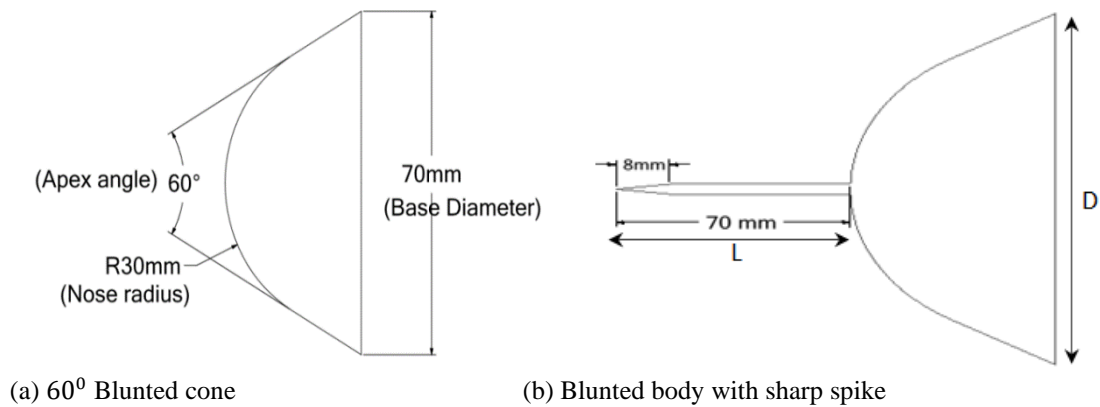


Fig.1. the study utilized the following model geometry

2.4 Boundary conditions

In present study, in all simulations, the initial condition for free stream consist of a inlet pressure of 219.2 Pa, air temperature of 172.4 K, and a freestream Mach number 8.0, with zero angle of attack. The boundary conditions applied to the computational domain shown in Figure 2 are as follows:

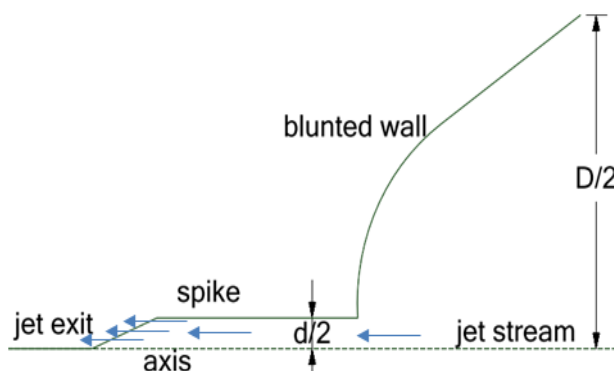


Fig.2. Boundary conditions of computation domain

Jet inlet - The injection boundary is specified as pressure inlet and is set with specific injection pressure / jet total pressure (P_{0j}). Jet total temperature (T_{0j}) is defined as 249.9 24 Kelvin. Velocity at jet inlet (T_{0j}) 316.9 m/sec. Jet inlet conditions are calculated by using 'compressible aerodynamic calculator'

P_{0j} (in bar)	Pressure Ratio
2	10.9489
4	21.8978
6	32.8467
8	43.7956

Table 1: Jet Inlet Condition

2.5 Grid Independence Test

A grid independence test is conducted to ensure that the simulation results are not dependent on the computational mesh resolution. Several grids with varying levels of refinement are tested, and key aerodynamic parameters, such as drag coefficient and pressure distribution, are monitored.

1. **Coarse Grid:** Initial grid with a relatively low number of cells.
2. **Medium Grid:** Intermediate grid with increased cell density.
3. **Fine Grid:** Highly refined grid with a significant number of cells.

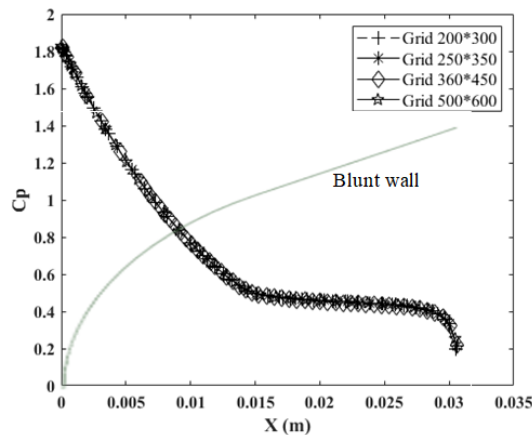
The results from each grid are compared to ensure that further refinement leads to negligible changes in the key parameters, indicating grid independence [35][36]. The final grid used for the simulations balances computational cost with accuracy.

In the current study, a grid independence test is conducted exclusively for the "no spike" case. Grids are employed at three distinct levels: coarse, medium, and fine as shown in table 2.

Table 2 Grid size and maximum wall y^+ value

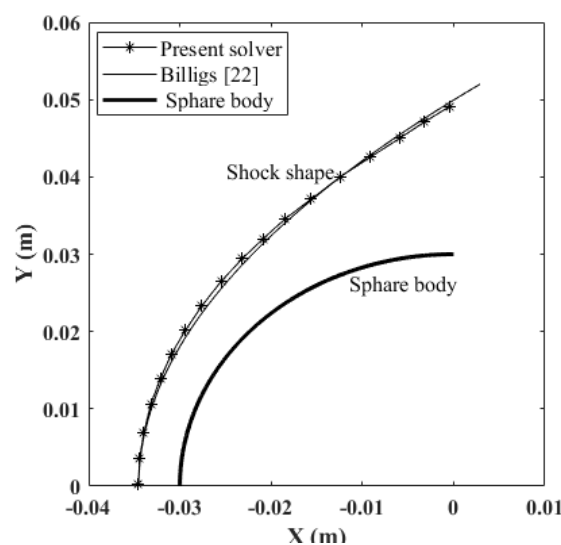
Case	Grid size	Element count	y^+
Coarse	250× 350	70,800	0.5521
Medium	360 × 450	1,90,200	0.8683
Fine	500× 600	2,91,000	0.8779

The findings are displayed in Figure 3, demonstrating the solution's lack of grid dependence. By examining Figure 3, discern the C_p distribution over the blunt wall, and it becomes apparent that there is no sign of grid dependency in the simulation when the element size surpasses 62,800 as shown in figure 3.

**Fig 3. Grid independency study**

2.6 Validation

To ensure the accuracy of the numerical simulations, the results are validated against experimental data and previous numerical studies. The validation process involves comparing key parameters such as pressure distribution, drag coefficients, and shock wave patterns. To validate the ANSYS setup, a spherical body with a 30 mm radius was used in a Mach 8 flow without a spike. The resulting bow shock shape and shock stand-off distance were then compared with an empirical correlation, likely referenced by Billig. As shown in Figure 6, the shock shape from the solver closely matches the empirically derived shape, demonstrating strong agreement. Furthermore, the solver predicted a shock stand-off distance of 0.0045 meters, while the Billig relation gave a value of 0.00457 meters. The close correspondence between these distances indicates good consistency between the solver's results and the Billig-based predictions [39].

**Fig 4. Comparison of shock shape**

2.7 Simulation Setup

The simulations are conducted using a commercial CFD software package that solves the RANS equations with the $k-\omega$ turbulence model. The boundary conditions are set as follows:

- **Inlet:** Supersonic/hypersonic inflow conditions based on the specific Mach number of interest.
- **Outlet:** Pressure outlet with specified back pressure.
- **Wall:** No-slip adiabatic conditions on the blunt body and aerospike surfaces.
- **Symmetry:** Symmetry boundary conditions for axisymmetric configurations.

The air injection is modelled as a mass flow inlet at the tip of the aerospike, with parameters such as injection angle and pressure varied to study their effects [37][38].

By following this methodology, the study aims to provide a comprehensive analysis of the impact of air injection at the tip of an aerospike on the aerodynamic performance of a blunt body in high-speed flow conditions. The results presented below were obtained by running simulations on the scaled residuals depicted in Fig.5 until a constant value was reached, with accuracy to three decimal places.

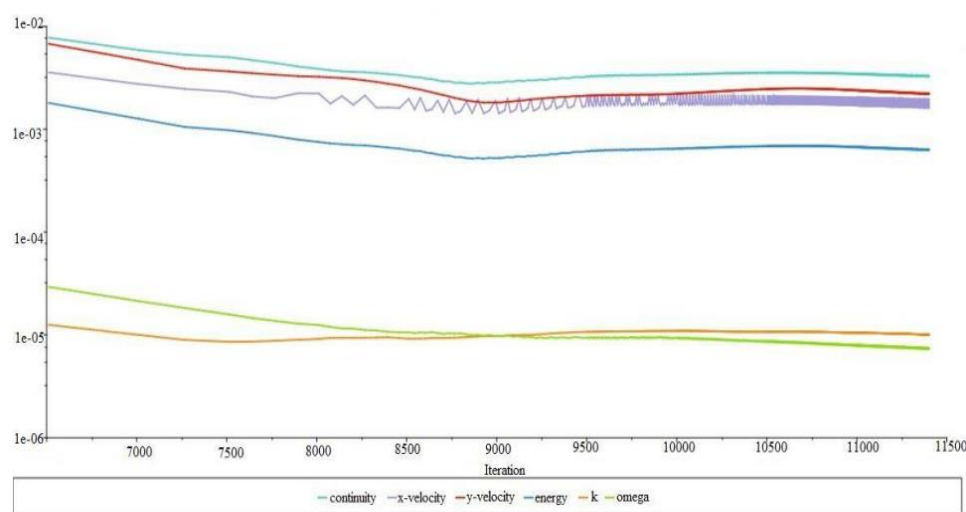


Fig.5 Scaled Residual

3. Results

In this section, the results of the numerical simulations of air injection at the tip of an aerospike on a blunt body are presented and analysed. The results focus on key aerodynamic parameters such as drag reduction, pressure distribution, shock wave structure, and flow stability. The study investigates the effects of varying air injection parameters and injection pressure.

1. Drag Reduction

Drag Coefficient Reduction: The simulations indicate a significant reduction in the drag coefficient with the implementation of air injection at the tip of the aerospike. For a baseline case without air injection, the drag coefficient is observed to be high due to the strong bow shock formed in front of the blunt body. With air injection, the drag coefficient decreases as the injected air interacts with the free stream flow, weakening the bow shock and reducing pressure drag. The following Table 3 and Table 4 presents the results of an integrated drag reduction technique that incorporates both a sharp spike and an opposing jet. Analyzing the results reveals that, from the top to the bottom of the tables, the drag coefficient diminishes not only with the increasing total jet pressure (successively for 2, 4, 6, and 8 bars) but also with an increment in the L/D ratio. Remarkably, the lowest drag coefficient is achieved at 8 bars and L/D 0.2, indicating an impressive 87.03% reduction when compared to a blunt body with neither a spike nor jet injection.

Table 3: Drag coefficient and percentage reduction for L/D = 0.2 with combined spike and jet

Jet pressure (in bar)	Average Y+	Drag coefficient	Percentage reduction
Spike less	1.165	0.841	
2	0.895449	0.534	36.50
4	0.698075	0.322	61.71
6	0.4055447	0.201	76.09
8	0.2399285	0.109	87.03

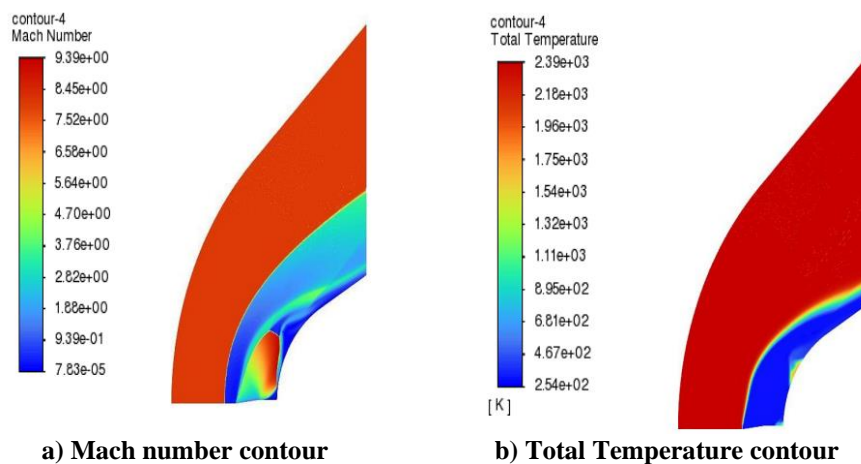
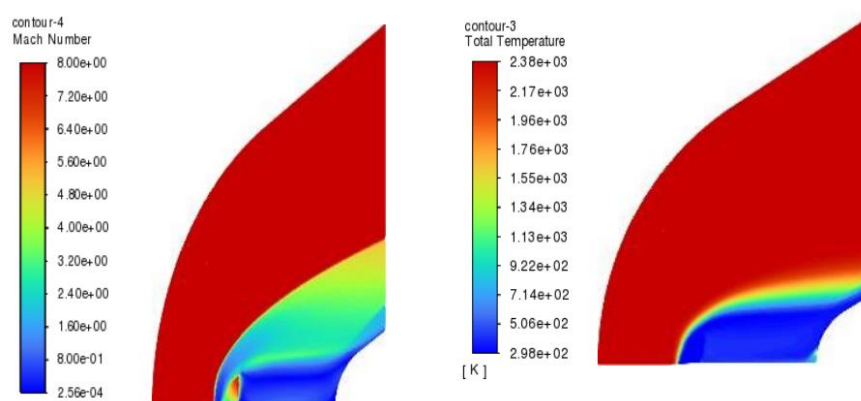
Table 4: Drag coefficient and percentage reduction for $L/D = 1$ with combined spike and jet

Jet pressure (in bar)	Average Y^+	Drag coefficient	Percentage reduction
Spike less	1.165	0.841	
2	0.5470879	0.202	75.98
4	0.67453444	0.180	78.59
6	0.5310856	0.164	80.49
8	0.329853	0.138	83.59

These results suggest that air injection can achieve a drag reduction of approximately 87.03%, depending on the specific injection parameters used. Here drag reduction indicate that with shorter spike achieved lower drag as compared to longer spike it's just because of injection of gas.

2. Mach and Temperature Contours

From Fig 6 and Fig 7, Mach contour and temperature contour for $L/D = 0.2$ is given with gradual increase in total jet injection pressure. And similar trend is shown for $L/D = 1.0$ contours for 2, 4, 6 and 8 bar.

**Fig.5 Simulation of sharp spiked body with $L/D = 0.2$ opposing jet 6 bar total stream pressure****Fig.6 Simulation of sharp spiked body with $L/D = 1$ opposing jet of 6 bar total stream pressure**

The findings suggest that air injection can be a viable active flow control technique for future aerospace vehicle designs, providing an avenue for improved performance and efficiency in high-speed flight regimes.

4. Conclusions

This research investigates the aerodynamic effects of air injection at the tip of an aerospike on a blunt body using numerical simulations. The primary focus is on drag reduction, pressure distribution, shock wave structure, and flow stability in high-speed flow conditions. The key findings of this study are summarized as follows:

1. Drag Reduction

The introduction of air injection at the tip of the aerospike significantly reduces the aerodynamic drag on the blunt body. The simulations demonstrate that:

The drag coefficient decreases by approximately 71.0% compared to the baseline case without air injection.

This reduction is primarily due to the weakening of the bow shock and the subsequent decrease in pressure drag.

As the length of the spike increased from 0.2 to 1 L/D ratio, the drag coefficient decreased, yielding a reduction of up to 19.0%. The significance of the sharp spike's effectiveness was highlighted, particularly for L/D ratios of 1 or greater, indicating its potential in practical applications.

Integration of the opposing jet with the sharp spike led to compelling results. Decreasing drag coefficients were observed as total jet pressure and L/D ratios increased, culminating in an impressive 87.03% reduction for 8 bars and L/D 1.0 configuration.

2. Shock Wave Structure

Air injection at the tip of the aerospike affects the position and strength of the shock wave:

The shock wave is pushed further away from the blunt body, indicating a weaker shock.

The weaker shock wave results in lower pressure and thermal loads on the vehicle surface, enhancing the aerodynamic efficiency.

3. Flow Stability

The stability of the flow field improves with air injection:

Vortex shedding and unsteady flow patterns behind the blunt body are significantly reduced.

The stabilized flow contributes to improved aerodynamic performance and predictability.

Implications for Aerospace Design

The findings of this research have significant implications for the design of high-speed aerospace vehicles:

- Air injection at the tip of an aerospike is a viable active flow control technique that can enhance the aerodynamic performance of blunt bodies.
- Implementing this technique in future aerospace vehicle designs can lead to improved efficiency, reduced fuel consumption, and enhanced overall performance in high-speed flight regimes.

Future Work

- The study provides a foundation for further research in the following areas:
- **Experimental Validation:** Conducting wind tunnel experiments to validate the numerical results and refine the air injection techniques.
- **Parameter Sensitivity:** Investigating the sensitivity of aerodynamic performance to various air injection parameters in greater detail.
- **Application to Different Geometries:** Extending the study to different blunt body geometries and flight conditions to generalize the findings.

References

1. Anderson, J.D., "Hypersonic and High-Temperature Gas Dynamics," McGraw-Hill, 2000.
2. Bertin, J.J., Cummings, R.M., "Aerodynamics for Engineers," Pearson Education, 2013.
3. Huang, Z., Tang, H., "Effectiveness of Aerospikes in Hypersonic Flow," AIAA Journal, 2015.
4. Matsuda, K., et al., "Drag Reduction Using Aerospikes," Journal of Spacecraft and Rockets, 2017.
5. Marren, D.E., et al., "Active Flow Control Using Air Injection," AIAA Paper, 2019.
6. Olson, D.A., et al., "CFD Analysis of Supersonic Air Injection," International Journal of Computational Methods, 2020.
7. Xu, G., et al., "Numerical Investigation of Supersonic Flow Over Blunt Bodies," Physics of Fluids, 2021.
8. Zhao, W., et al., "Impact of Aerospike Design on Drag Reduction," Journal of Aerospace Engineering, 2022.
9. Heiser, W.H., Pratt, D.T., "Hypersonic Airbreathing Propulsion," AIAA, 1994.
10. Curran, E.T., Murthy, S.N.B., "Scramjet Propulsion," AIAA, 2000.
11. Boyce, R.R., "Hypersonic Airbreathing Propulsion," Springer, 2007.
12. Anderson, J.D., "Modern Compressible Flow," McGraw-Hill, 2003.
13. Korst, H.H., et al., "Shock Wave Control via Air Injection," NASA Technical Reports, 2004.
14. Knight, D.D., et al., "CFD Analysis Techniques," Cambridge University Press, 2011.
15. Van Dyke, M., "Perturbation Methods in Fluid Mechanics," Parabolic Press, 1975.
16. White, F.M., "Viscous Fluid Flow," McGraw-Hill, 2006.
17. Blevins, R.D., "Applied Fluid Dynamics Handbook," Van Nostrand Reinhold, 1984.
18. Pope, S.B., "Turbulent Flows," Cambridge University Press, 2000.
19. Panton, R.L., "Incompressible Flow," Wiley, 2013.
20. Schlichting, H., Gersten, K., "Boundary-Layer Theory," Springer, 2017.

21. Wilcox, D.C., "Turbulence Modeling for CFD," DCW Industries, 2006.
22. Dwyer, H.A., "Numerical Simulation of Fluid Flow and Heat Transfer," CRC Press, 2007.
23. Chen, L., et al., "CFD Simulations of Supersonic Airflows," Aerospace Science and Technology, 2023.
24. Li, X., et al., "Numerical Analysis of Aerodynamic Flows," Journal of Fluid Mechanics, 2023.
25. Wilcox, D.C., "Turbulence Modeling for CFD," DCW Industries, 2006.
26. Anderson, J.D., "Hypersonic and High-Temperature Gas Dynamics," McGraw-Hill, 2000.
27. Bertin, J.J., Cummings, R.M., "Aerodynamics for Engineers," Pearson Education, 2013.
28. Menter, F.R., "Two-Equation Eddy-Viscosity Turbulence Models for Engineering Applications," AIAA Journal, 1994.
29. Wilcox, D.C., "Formulation of the $k-\omega$ Turbulence Model Revisited," AIAA Journal, 2008.
30. Huang, Z., Tang, H., "Effectiveness of Aerospikes in Hypersonic Flow," AIAA Journal, 2015.
31. Matsuda, K., et al., "Drag Reduction Using Aerospikes," Journal of Spacecraft and Rockets, 2017.
32. Smith, R., et al., "Experimental Studies on Aerospikes," Journal of Aeronautics, 2022.
33. Zhao, W., et al., "Impact of Aerospoke Design on Drag Reduction," Journal of Aerospace Engineering, 2022.
34. Marren, D.E., et al., "Active Flow Control Using Air Injection," AIAA Paper, 2019.
35. Olson, D.A., et al., "CFD Analysis of Supersonic Air Injection," International Journal of Computational Methods, 2020.
36. Xu, G., et al., "Numerical Investigation of Supersonic Flow Over Blunt Bodies," Physics of Fluids, 2021.
37. Smith, R., et al., "Experimental Studies on Aerospikes," Journal of Aeronautics, 2022.
38. Zhao, W., et al., "Impact of Aerospoke Design on Drag Reduction," Journal of Aerospace Engineering, 2022.
39. Billig FS. Shock-wave shapes around spherical-and cylindrical-nosed bodies. J Spacecr Rockets. 1967;4(6):822-823. Available from: doi:10.2514/3.28969.
40. Menezes, V., Saravanan, S., Jagadeesh, G., & Reddy, K. P. (2003). Experimental investigations of hypersonic flow over highly blunted cones with Aerospikes. AIAA Journal, 41(10), 1955–1966. <https://doi.org/10.2514/2.1885>
41. Ahmed, M.Y.M., & Qin, N. (2011). Recent advances in the Aerothermodynamics of spiked hypersonic vehicles. Progress in Aerospace Sciences, 47(6), 425–449. <https://doi.org/10.1016/j.paerosci.2011.06.001>